Lectures on Cosmic Topological Defects

Tanmay Vachaspati
Department of Astronomy and Astrophysics,
T.I.F.R., Homi Bhabha Road,
Colaba, Mumbai 400 005, India
and
Physics Department,
Case Western Reserve University,
Cleveland, OH 44106-7079, USA.

These lectures review certain topological defects and aspects of their cosmology. Unconventional material includes brief descriptions of electroweak defects, the structure of domain walls in non-Abelian theories, and the spectrum of magnetic monopoles in SU(5) Grand Unified theory.

Contents

1 Introduction

1.1 FRW cosmology

As indicated by observations, the universe is assumed to be homogeneous and isotropic on large scales. The line element is:

$$ds^2 = dt^2 - a^2(t)\left[\frac{dr^2}{1-kr^2} + r^2(d\theta^2 + \sin^2\theta d\phi^2)\right] \tag{1}$$

where the function $a(t)$ is known as the scale factor, and the parameter $k = -1, 0, +1$ labels an open, flat or closed universe. The Einstein equations give:

$$\left(\frac{\dot{a}}{a}\right)^2 + \frac{k}{a^2} = \frac{8\pi G}{3}\rho(t) \tag{2}$$

where $\rho(t)$ is the energy density of the cosmological fluid. Conservation of energy-momentum yields

$$\dot{\rho} + 3H(\rho + p) = 0 \tag{3}$$

where $H \equiv \dot{a}/a$ is the Hubble parameter and p denotes the pressure of the cosmological fluid. The properties of the cosmological fluid are given by its equation of state:

$$p = p(\rho) \tag{4}$$

which must be specified to determine the expansion rate of the universe. If the fluid is relativistic (*eg.* photons): $p = \rho/3$; while if it is dust: $p = 0$; and for vacuum energy (cosmological constant): $p = -\rho$.

If the fluid is in thermal equilibrium, the evolution of the temperature of the fluid can be derived by using the conservation of entropy which gives

$$a(t)T = \text{constant} . \tag{5}$$

The temperature of the cosmic microwave background radiation (*i.e.* cosmological photons as opposed to those produced by stars and other astrophysical sources) at the present epoch is measured to be 2.7°K.

It is sometimes convenient to work with the "conformal time" τ instead of the "cosmic time" t. The relation defining τ in terms of t is:

$$dt = a(t)d\tau . \tag{6}$$

In terms of the conformal time, the FRW line element is:

$$ds^2 = a^2(t(\tau))\left[d\tau^2 - \frac{dr^2}{1-kr^2} + r^2(d\theta^2 + \sin^2\theta d\phi^2)\right] . \tag{7}$$

1.2 Cosmological phase transitions

We consider a field theory of scalar, spinor and vector fields:

$$L = L_B + L_F \tag{8}$$

with the bosonic Lagrangian:

$$L_B = \frac{1}{2} D_\mu \Phi_i D^\mu \Phi_i - V(\Phi) - \frac{1}{4} F^a_{\mu\nu} F^{\mu\nu a} \tag{9}$$

where Φ_i are the components of the scalar fields. The fermionic Lagrangian for a fermionic multiplet Ψ is:

$$L_F = i\bar{\Psi}\gamma^\mu D_\mu \Psi - \bar{\Psi}\Gamma_i \Psi \Phi_i \ . \tag{10}$$

In addition we have the following definitions:

$$D_\mu \equiv \partial_\mu - ieA^a_\mu T^a \tag{11}$$

where the T^a are group generators;

$$F^a_{\mu\nu} \equiv \partial_\mu A^a_\nu - \partial_\nu A^a_\mu + +ef^{abc} A^b_\mu A^c_\nu \tag{12}$$

where, A^a_μ are the gauge fields.

If the expectation values of the scalar fields are denoted by Φ_{0i}, then the mass matrices of the various fields are written as:

$$\mu^2_{ij} = \left. \frac{\partial^2 V}{\partial \Phi_i \partial \Phi_j} \right|_{\Phi = \Phi_0} , \quad \text{scalar fields} \tag{13}$$

$$m = \Gamma_i \Phi_{0i} \ , \quad \text{spinor fields} \tag{14}$$

where, the Γ_i are the Yukawa coupling matrices, and

$$M^2_{ab} = e^2 (T_a T_b)_{ij} \Phi_{0i} \Phi_{0j} \ , \quad \text{vector fields} \tag{15}$$

Then the finite temperature, one-loop effective potential is:

$$V_{eff}(\Phi_0, T) = V(\Phi_0) + \frac{\mathcal{M}^2}{24} T^2 - \frac{\pi^2}{90} \mathcal{N} T^4 \tag{16}$$

where

$$\mathcal{N} = \mathcal{N}_B + \frac{7}{8} \mathcal{N}_F \tag{17}$$

is the number of bosonic and fermionic spin states, and

$$\mathcal{M}^2 = \mathrm{Tr}\mu^2 + 3\mathrm{Tr}M^2 + \frac{1}{2}\mathrm{Tr}(\gamma^0 m \gamma^0 m) \ . \tag{18}$$

Note that $\mathcal{M}^2$ depends on the expectation value Φ_0 through the defining equations for the mass matrices given above. Then, for example, $\mathcal{M}^2$ will contain a term proportional to $\mathrm{Tr}(\Phi_0^2)$.

For us the important feature of the effective potential is that it can lead to cosmological phase transitions. If there are scalar fields with negative mass squared terms in $V(\Phi)$, the contributions from the $\mathcal{M}^2 T^2$ term in the effective potential can make the effective mass squared positive for these fields if the temperature is high enough. Therefore when the universe is at a high temperature, the effective squared mass is positive and the minimum of the potential is at $\Phi_0 = 0$. In the more recent cooler universe the effective mass squared is negative and the minima of the effective potential will occur at non-zero values of Φ_0. That is, the scalar fields will acquire vacuum expectation values. This is the phenomenon of spontaneous symmetry breaking and, if it occurs, will manifest itself as a cosmological phase transition.

1.3 Vacuum manifold

In general the field theoretic action under consideration will be invariant under some transformations of the fields. The set of all such symmetry transformations form a group which we denote by G.

Next consider the situation where a scalar field acquires a vacuum expectation value (VEV) ϕ_0. Then all transformations of ϕ_0 by elements of G will also be legitimate VEVs of the scalar field. However, not all elements of G will have a non-trivial effect on ϕ_0. There will be a subgroup of G which will have a trivial action on ϕ_0. This is the unbroken subgroup of G and we denote it by H.

Now we wish to determine the set of possible VEVs of the scalar field. This set is given by the elements of G that have a non-trivial action on ϕ_0. Now consider an element of $g \in G$ that has a non-trivial action on ϕ_0 and transforms it to ϕ_1. Then every element of the form gh where $h \in H$, also takes ϕ_0 to ϕ_1. Therefore the non-trivial transformations are given by the left cosets of H, and the space of all non-trivial transformations is called a coset space and denoted by G/H. Therefore the vacuum manifold of the theory is G/H.

As we shall see, topological defects occur due to non-trivial topology of the vacuum manifold.

Note that the topology does not care if the symmetries are local or global. For most of these lectures, I will consider local (gauged) symmetries.

2 Domain walls

2.1 Topology: π_0

Domain walls occur when the vacuum manifold has two or more disconnected components. For example, G can be a discrete group like Z_2 which can be broken completely ($H = \mathbf{1}$). Then G/H consists of just two points.

The topology of various manifolds has been studied by mathematicians and they characterize the type of topology by stating the homotopy groups of the manifold. The n^{th} homotopy group of the manifold G/H is denoted by $\pi_n(G/H)$ and denotes the group that is formed by considering the mapping of $n-$dimensional spheres into the manifold G/H. Each element of the group π_n is the set of mappings that can be continuously deformed into one another.

In the case when the vacuum manifold has disconnected components, $\pi_0(G/H)$ is non-trivial since there are points (zero dimensional spheres) that lie in different components that cannot be continuously deformed into one another. Therefore domain walls occur whenever $\pi_0(G/H)$ is non-trivial.

2.2 Example: Z_2

Consider the Z_2 Lagrangian in 1+1 dimensions labeled by (t, z)

$$L = \frac{1}{2}(\partial_\mu \phi)^2 - \frac{\lambda}{4}(\phi^2 - \eta^2)^2 \tag{19}$$

where $\phi(t, z)$ is a real scalar field - also called the order parameter. The Lagrangian is invariant under $\phi \to -\phi$ and hence possesses a Z_2 symmetry. For this reason, the potential has two minima: $\phi = \pm\eta$, and the "vacuum manifold" has two-fold degeneracy.

Consider the possibility that $\phi = +\eta$ at $z = +\infty$ and $\phi = -\eta$ at $z = -\infty$. In this case, the continuous function $\phi(z)$ has to go from $-\eta$ to $+\eta$ as z is taken from $-\infty$ to $+\infty$ and so must necessarily pass through $\phi = 0$. But then there is energy in this field configuration since the potential is non-zero when $\phi = 0$. Also, this configuration cannot relax to either of the two vacuum configurations, say $\phi(z) = +\eta$, since that involves changing the field over an infinite volume from $-\eta$ to $+\eta$, which would cost an infinite amount of energy.

Another way to see this is to notice the presence of a conserved current:

$$j^\mu = \epsilon^{\mu\nu}\partial_\nu \phi$$

where $\mu, \nu = 0, 1$ and $\epsilon^{\mu\nu}$ is the antisymmetric symbol in 2 dimensions. Clearly j^μ is conserved and so we have a conserved charge in the model:

$$Q = \int dz j^0 = \phi(+\infty) - \phi(-\infty) \ .$$

For the vacuum $Q = 0$ and for the configuration described above $Q = 1$. So the configuration cannot relax into the vacuum - it is in a different topological sector.

To get the field configuration with the boundary conditions $\phi(\pm\infty) = \pm\eta$, one would have to solve the field equation resulting from the Lagrangian (19). This would be a second order differential equation. Instead, one can use the clever method first derived by Bogomolnyi[1] and obtain a first order differential equation. The method uses the energy functional:

$$\begin{aligned} E &= \int dz[\frac{1}{2}(\partial_t\phi)^2 + \frac{1}{2}(\partial_z\phi)^2 + V(\phi)] \\ &= \int dz[\frac{1}{2}(\partial_t\phi)^2 + \frac{1}{2}(\partial_z\phi - \sqrt{2V(\phi)}\ )^2 + \sqrt{2V(\phi)}\partial_z\phi] \\ &= \int dz[\frac{1}{2}(\partial_t\phi)^2 + \frac{1}{2}(\partial_z\phi - \sqrt{2V(\phi)}\ )^2] + \int_{\phi(-\infty)}^{\phi(+\infty)} d\phi' \sqrt{2V(\phi')} \end{aligned}$$

Then, for fixed values of ϕ at $\pm\infty$, the energy is minimized if

$$\partial_t\phi = 0$$

and

$$\partial_z\phi - \sqrt{2V(\phi)} = 0 \ .$$

Furthermore, the minimum value of the energy is:

$$E_{min} = \int_{\phi(-\infty)}^{\phi(+\infty)} d\phi' \sqrt{2V(\phi')} \ .$$

In our case,

$$\sqrt{V(\phi)} = \sqrt{\frac{\lambda}{4}}(\eta^2 - \phi^2)$$

which can be inserted in the above equations to get the "kink" solution:

$$\phi = \eta \tanh\left(\sqrt{\frac{\lambda}{2}}\eta z\right)$$

for which the energy per unit area is:

$$\sigma_{kink} = \frac{2\sqrt{2}}{3}\sqrt{\lambda}\eta^3 = \frac{2\sqrt{2}}{3}\frac{m^3}{\sqrt{\lambda}} \tag{20}$$

where $m = \sqrt{\lambda}\eta$ is the mass scale in the model (see eq. (19)). Note that the energy density is localized in the region where ϕ is not in the vacuum, *i.e.* in a region of thickness $\sim m^{-1}$ around $z = 0$.

We can extend the model in eq. (19) to 3+1 dimensions and consider the case when ϕ only depends on z but not on x and y. We can still obtain the kink solution for every value of x and y and so the kink solution will describe a "domain wall" in the $xy-$plane.

At the center of the kink, $\phi = 0$, and hence the Z_2 symmetry is restored in the core of the kink. In this sense, the kink is a "relic" of the symmetric phase of the system. If kinks were present in the universe today, their interiors would give us a glimpse of what the universe was like prior to the phase transition.

2.3 SU(5)

An example that is more relevant to cosmology is motivated by Grand Unification. Here we will consider the SU(5) model:

$$L = \mathrm{Tr}(D_\mu\Phi)^2 - \frac{1}{2}\mathrm{Tr}(X_{\mu\nu}X^{\mu\nu}) - V(\Phi) \tag{21}$$

where, in terms of components, $\Phi = \Phi^a T^a$ is an SU(5) adjoint, the gauge field strengths are $X_{\mu\nu} = X^a_{\mu\nu}T^a$ and the SU(5) generators T^a are normalized such that $\mathrm{Tr}(T^aT^b) = \delta^{ab}/2$. The definition of the covariant derivative is:

$$D_\mu\Phi = \partial_\mu\Phi - ie[X_\mu, \Phi] \tag{22}$$

and the potential is the most general quartic in Φ:

$$V(\Phi) = -m^2\mathrm{Tr}(\Phi^2) + h[\mathrm{Tr}(\Phi^2)]^2 + \lambda\mathrm{Tr}(\Phi^4) + \gamma\mathrm{Tr}(\Phi^3) - V_0\ , \tag{23}$$

where, V_0 is a constant that we will choose so as to set the minimum value of the potential to zero.

The $SU(5)$ symmetry is broken to $[SU(3)\times SU(2)\times U(1)]/Z_6$ if the Higgs acquires a VEV equal to

$$\Phi_0 = \frac{\eta}{2\sqrt{15}}\mathrm{diag}(2,2,2,-3,-3) \tag{24}$$

where

$$\eta = \frac{m}{\sqrt{\lambda'}} \ , \quad \lambda' \equiv h + \frac{7}{30}\lambda \ . \tag{25}$$

For the potential to have its global minimum at $\Phi = \Phi_0$, the parameters are constrained to satisfy:

$$\lambda \geq 0 \ , \quad \lambda' \geq 0 \ . \tag{26}$$

For the global minimum to have $V(\Phi_0) = 0$, in eq. (23) we set

$$V_0 = -\frac{\lambda'}{4}\eta^4 \ . \tag{27}$$

The model in eq. (21) does not have any topological domain walls because there are no broken discrete symmetries. In particular, the Z_2 symmetry under $\Phi \to -\Phi$ is absent due to the cubic term. However if γ is small, there are walls connecting the two vacua related by $\Phi \to -\Phi$ that are almost topological. In our analysis we will set $\gamma = 0$, in which case the symmetry of the model is $SU(5) \times Z_2$ and an expectation of Φ breaks the Z_2 symmetry leading to topological domain walls.

The kink solution is the Z_2 kink along the Φ_0 direction (see eq. (24)). Therefore:

$$\Phi_k = \tanh(\sigma z)\Phi_0 \tag{28}$$

with $\sigma \equiv m/\sqrt{2}$ (see eq. (25)), and all the gauge fields vanish. It is straightforward to check that Φ_k solves the equations of motion with the boundary conditions $\Phi(z = \pm\infty) = \pm\Phi_0$.

The energy per unit area of the kink is (see eq. (20)):

$$M_k = \frac{2\sqrt{2}}{3}\frac{m^3}{\lambda'} \ . \tag{29}$$

The existence of a static solution to the equations of motion only guarantees that it is an extremum of the energy but this extremum may not be a minimum. To determine if the kink is a minimum energy solution we need to examine its stability under arbitrary perturbations. (As far as I know, a Bogomolnyi type analysis has not been constructed for the SU(5) model.)

Here we will examine the stability of the kink under general perturbations. So we write:

$$\Phi = \Phi_k + \Psi \tag{30}$$

Since the kink solution is invariant under translations and rotations in the $xy-$plane, it is easy to show that the perturbations that might cause an instability arise from perturbations of the scalar field and can only depend on z. Therefore we may set the gauge fields to zero and take $\Psi = \Psi(t, z)$.

The Z_2 kink is stable and hence we can restrict the scalar perturbations to be orthogonal to Φ_k. The perturbative stability of the kink has been studied by *Dvali et. al.* [2], and, *Pogosian and Vachaspati* [3]. Here we only consider the off-diagonal perturbation

$$\Psi = \psi T \equiv \psi \mathrm{diag}(\tau^1, 0, 0, 0) \ , \tag{31}$$

where τ^1 is the first Pauli spin matrix.

Next we analyze the linearized Schrodinger equation for small excitations $\psi = \psi_0(z) exp(-i\omega t)$ in the background of the kink:

$$[-\partial_z^2 - m^2 + \phi_k^2(z)(h + \lambda r)]\psi_0 = \omega_i^2 \psi_0 \ \ , \tag{32}$$

where $\phi_k \equiv \tanh(\sigma z)$ and $r = 7/30$. The kink is unstable if there is a solution to eq. (32) with a negative ω^2. Substituting eq. (28) into eq. (32) yields:

$$[-\partial_z^2 + m^2(\tanh^2(\sigma z) - 1)]\psi_0 = \omega^2 \psi_0 \ \ . \tag{33}$$

This equation has a bound state solution $\psi_0 \propto \mathrm{sech}(\sigma z)$ with the eigenvalue $\omega^2 = -m^2/2$. Since this result is independent of the parameters in the potential, we conclude that the kink in SU(5) is always unstable.

So we still need to find the topological domain wall solution in the model.

The domain wall solution is obtained if we choose the gauge fields to vanish at infinity and the scalar field to satisfy the boundary conditions:

$$\begin{aligned}\Phi(z = -\infty) = \Phi^- &\equiv \frac{\eta}{2\sqrt{15}} \mathrm{diag}(3, -2, -2, 3, -2) \\ &= \eta \sqrt{\frac{5}{12}} (\lambda_3 + \tau_3) - \frac{\eta}{6} (Y - \sqrt{5}\lambda_8)\end{aligned} \tag{34}$$

and

$$\begin{aligned}\Phi(z = +\infty) = \Phi^+ &\equiv \frac{\eta}{2\sqrt{15}} \mathrm{diag}(2, -3, 2, 2, -3) \\ &= \eta \sqrt{\frac{5}{12}} (\lambda_3 + \tau_3) + \frac{\eta}{6} (Y - \sqrt{5}\lambda_8) \ .\end{aligned} \tag{35}$$

Here λ_3, λ_8, τ_3 and Y are the diagonal generators of SU(5):

$$\lambda_3 = \frac{1}{2} \mathrm{diag}(1, -1, 0, 0, 0) \ , \tag{36}$$

$$\lambda_8 = \frac{1}{2\sqrt{3}} \mathrm{diag}(1, 1, -2, 0, 0) \ , \tag{37}$$

$$\tau_3 = \frac{1}{2}\mathrm{diag}(0,0,0,1,-1) \ , \tag{38}$$

$$Y = \frac{1}{2\sqrt{15}}\mathrm{diag}(2,2,2,-3,-3) \ . \tag{39}$$

Alternately, we could have chosen the boundary conditions to be like those of the kink with $\Phi(z=+\infty) = -\Phi(z=-\infty)$. However, then the solution for the domain wall will not be diagonal at all z. We prefer to use the above boundary conditions so that the solution is diagonal throughout.

The domain wall solution can be written as

$$\Phi_{DW}(z) = a(z)\lambda_3 + b(z)\lambda_8 + c(z)\tau_3 + d(z)Y \ . \tag{40}$$

The functions a, b, c, and d must satisfy the static equations of motion:

$$\begin{aligned} a'' = [-m^2 + (h + \frac{2\lambda}{5})d^2 \quad &+ \quad (h + \frac{\lambda}{2})(a^2+b^2) + hc^2]a \\ &+ \quad \frac{2\lambda abd}{\sqrt{5}} \end{aligned} \tag{41}$$

$$\begin{aligned} b'' = [-m^2 + (h + \frac{2\lambda}{5})d^2 \quad &+ \quad (h + \frac{\lambda}{2})(a^2+b^2) + hc^2]b \\ &+ \quad \frac{\lambda d}{\sqrt{5}}(a^2 - b^2) \end{aligned} \tag{42}$$

$$\begin{aligned} c'' = [-m^2 + (h + \frac{9\lambda}{10})d^2 + (h \quad &+ \quad \frac{\lambda}{2})c^2 \\ &+ \quad h(a^2+b^2)]c \end{aligned} \tag{43}$$

$$\begin{aligned} d'' = [-m^2 \quad &+ \quad (h + \frac{7\lambda}{30})d^2 + (h + \frac{2\lambda}{5})(a^2+b^2) \\ &+ \quad (h + \frac{9\lambda}{10})c^2]d + \frac{\lambda b}{\sqrt{5}}(a^2 - \frac{b^2}{3}) \ , \end{aligned} \tag{44}$$

where primes refer to derivatives with respect to z. For reference, the kink solution (eq. (28)) corresponds to $a(z) = 0 = b(z) = c(z)$ and $d(z) = \eta\tanh(\sigma z)$.

The equations of motion for b and c and can be solved quite easily:

$$b(z) = -\sqrt{5}d(z) \ , \quad c(z) = a(z) \ . \tag{45}$$

This is consistent with the boundary conditions in eqs. (34) and (35). In addition, we require

$$a(z = \pm\infty) = +\eta\sqrt{\frac{5}{12}} \ , \quad d(z = \pm\infty) = \pm\frac{\eta}{6} \ . \tag{46}$$

Then the remaining equations can be written in a cleaner form by rescaling:

$$A(z) = \sqrt{\frac{12}{5}}\frac{a}{\eta} \ , \quad D(z) = 6\frac{d}{\eta} \ , \quad Z = mz \ . \tag{47}$$

This leads to

$$A'' = \left[-1 + \frac{(1-p)}{5}D^2 + \frac{(4+p)}{5}A^2\right]A \tag{48}$$

$$D'' = \left[-1 + pD^2 + (1-p)A^2\right]D \tag{49}$$

where primes on A and D denote differentiation with respect to Z, and

$$p = \frac{1}{6}\left[1 + \frac{5\lambda}{12\lambda'}\right] \ . \tag{50}$$

Note that $p \in [1/6, \infty)$ because of the constraints in eq. (26). The boundary conditions now are:

$$A(z = \pm\infty) = +1 \ , \quad D(z = \pm\infty) = \pm 1 \ . \tag{51}$$

This system of equations has been solved by numerical relaxation and a sample solution is shown in Fig. 1. To find an approximate analytical solution, assume that $|A''/A| << 1$ is small everywhere. This assumption will be true for a certain range of the parameter p which we can later determine. Then the square bracket on the right-hand side of eq. (48) is very small. This gives:

$$A \simeq \left[\frac{5}{4+p}\left\{1 - \frac{(1-p)}{5}D^2\right\}\right]^{1/2} \tag{52}$$

We insert this expression for A in eq. (49) and obtain the kink-type differential equation:

$$D'' = q[-1 + D^2]D \ , \tag{53}$$

where

$$q = \frac{6p-1}{p+4} = \frac{6\lambda}{\lambda + 60\lambda'} \tag{54}$$

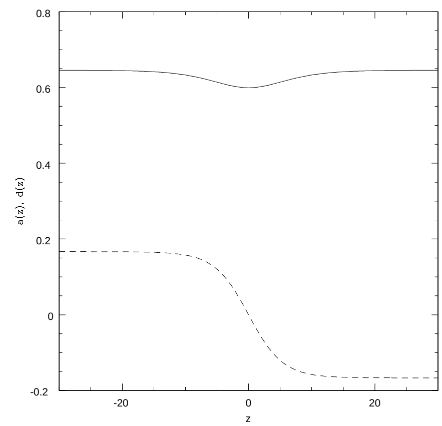

Figure 1: Numerical solution for the domain wall in the case $\lambda = 1$, $h = -0.2$ ($p = 2.25$). The solid line shows $a(z)$ and the dashed line shows $d(z)$.

and the solution is:

$$D(Z) \simeq \tanh\left(\sqrt{\frac{q}{2}}Z\right) \tag{55}$$

The parameter q lies in the interval $[0, 6]$. For $q = 1$ (*i.e.* $p = 1$) it is easy to check that this analytical solution is exact.

We can now check that our assumption $|A''/A| << 1$ is self-consistent provided p is not much larger than a few.

The energy density for the fields A and D can be found from the Lagrangian in eq. (21) together with the ansatz in eq. (40), the solution for b and c in eq. (45) and the rescalings in eq. (47). The resulting expression for the energy per unit area of the domain wall is:

$$M_{DW} = \frac{m^3}{12\lambda'} \int dZ [5{A'}^2 + {D'}^2 + V(A, D)] \tag{56}$$

where,

$$\begin{aligned} V(A, D) = -5A^2 \quad &- \quad D^2 + \frac{(p+4)}{2}A^4 \\ &+ \quad \frac{p}{2}D^4 + (1-p)A^2D^2 + 3 \ . \end{aligned} \tag{57}$$

Table 1: Size distribution of + clusters found by simulations on a cubic lattice.

Cluster size	1	2	3	4	6	10	31082
Number	462	84	14	13	1	1	1

The energy can be found numerically. However, here we will find an approximate analytic result. We can insert the approximate solution given above in eq. (56) but this leads to an expression that is not transparent. Instead it is more useful to consider another approximation for A and D:

$$A \simeq 1 \ , \quad D \simeq \tanh\left(\sqrt{\frac{p}{2}} Z\right) \ . \tag{58}$$

(This approximation is exact for $p = 1$.) A straightforward evaluation then gives:

$$M_{DW approx} = M_k \frac{\sqrt{p}}{6} \tag{59}$$

where, M_k is given in eq. (29).

It can be shown for a range of parameters that this domain wall solution is perturbatively stable. Numerically we find that it is lighter than the kink for all values of p. (Eq. (59) shows it to be lighter for $p < 36$.)

The interior of the domain wall has less symmetry than the exterior. So the domain wall does not contain a trapped region of the early universe. Instead it is a region that may be to our future where the $SU(3)$ symmetry is broken down to $SU(2) \times U(1)$. In this sense, the domain wall is a relic from the early universe but not a relic of the unbroken symmetry of the theory.

2.4 Formation

The properties of the network of domain walls at formation has been determined by numerical simulations. The idea behind the simulations is that the vacuum in any correlated region of space is determined at random. Then, if there are only two degenerate vacuua (call them + and -), there will be spatial regions that will be in the + phase and others in the - phase. The boundaries between these regions of different phases is the location of the domain walls.

By performing numerical simulations, the statistics shown in Table I was obtained [4].

The data shows that there is essentially one giant connected + cluster. By symmetry there will be one connected - cluster. In the infinite volume limit, these clusters will also be infinite and their surface areas will also be infinite. Therefore the topological domain wall formed at the phase transition will be infinite.

2.5 Evolution

Once the inifinite domain wall forms, it tries to straighten out since it has tension – in this way, the wall can minimize its energy. In the cosmological setting, the wall will be stretched out by the Hubble expansion. In addition, the wall will interact with the ambient matter and suffer friction. Sometimes different parts of the walls will collide and interact. The interaction leads to the reconnection of colliding walls.

The details of the evolution of the walls are quite complicated. However, the simplest cosmological scenario is easy to analyze and leads to an interesting bound. The basic idea is to use causality to get an upper bound on the energy density in domain walls at any epoch. Causality tells us that the different domains that are separated by walls cannot smooth out faster than the speed of light. Therefore every causal horizon must contain at least one domain wall at any epoch and so the energy density in domain walls ρ_{DW} obeys the following bound:

$$\rho_{DW} \geq \frac{\text{energy in one wall in horizon}}{\text{horizon volume}} \simeq \frac{\sigma t^2}{t^3} = \frac{\sigma}{t} \qquad (60)$$

where σ is the energy per unit area of the wall. If we require that the energy density in walls be less than the present critical density of the universe $\rho_{cr} = 3H^2/8\pi G$ with $H \simeq 70$ km/s/Mpc we get the constraint

$$\sigma < \frac{3H^2 t_0}{8\pi G} \ , \qquad (61)$$

where $t_0 \sim 10^{17}$ secs is the present epoch.

If we use eq. (20) to connect σ to the symmetry breaking scale and take the coupling constant to be order one, we find that the symmetry breaking scale is constrained to be less than about a GeV. A stronger bound is obtained by realizing that the energy density fluctuations in domain walls should not cause fluctuations in the cosmic microwave background radiation (CMBR) greater than 1 part in 10^5. This leads to the constraint that η should be less than a few MeV. Particle physics at such low energy scales – such as the standard model – do not show any phase transitions involving domain walls and so we

do not expect to have domain walls in the universe. Another way to view the constraint is that if a particle physics model predicts domain walls above the few MeV scale, cosmology rules out the model.

2.6 Further complexities

One can evade the constraints derived in the previous section by introducing some new cosmological and particle physics elements.

For example, the constraint that domain walls have to be formed below the few MeV scale does not hold if cosmological inflation follows the phase transition in which heavy domain walls were produced. In such a scenario, the domain walls are inflated away and our present horizon need not contain any domain wall.

In particle physics model building, one might have a situation where a discrete symmetry is broken at some high temperature and then restored at some lower temperature. In this case, heavy domain walls would be formed at the first phase transition and then would "dissolve" at the second phase transition. Then there would be a period in the early universe where domain walls would be present but they would not be around today.

Another situation of some interest is when the discrete vacuua are not exactly degenerate. In the SU(5) example discussed above, if γ (eq. (23)) is very small, domain walls will be formed at the phase transition. Suppose the + phase has slightly less energy density than the - phase. Then the domain walls will experience a pressure on them that will drive them towards the higher energy - phase. However, if γ is small, this pressure difference is also small and is negligible for the early evolution of the wall system. Only after the walls have straightened out to an extent that the curvature forces are less than the pressure, will the pressure start to drive the walls and eventually eliminate them.

3 Strings

3.1 Topology: π_1

If the vacuum manifold has one dimensional closed paths that cannot be contracted, there are topological string solutions in the field theory. The homotopy group $\pi_1(G/H)$ is the group formed by the equivalence classes of paths that can be deformed into each other and the group operation joins two paths to get another path. Each element of $\pi_1(G/H)$ labels a topologically distinct string solution.

An example of a field theory in which string solutions exist is based on a $U(1)$ (global or local) group which is broken down completely. The coset space $U(1)/\mathbf{1}$ is a one dimensional sphere (circle). Closed paths that wrap around the circle cannot be contracted to a point and this implies that the $U(1)$ model contains string solutions.

The $U(1)$ model is very important as it is relevant to the simplest superfluids and superconductors. However, in more complicated systems the symmetry groups are larger and calculating the homotopy group can be more involved. Fortunately there is a result that simplifies matters immensely for most (though not all!) particle physics applications. This is the result that if $\pi_n(G)$ and $\pi_{n-1}(G)$ are both trivial then,

$$\pi_n(G/H) = \pi_{n-1}(H) \ . \tag{62}$$

With $n = 1$ this gives

$$\pi_1(G/H) = \pi_0(H) \tag{63}$$

provided $\pi_1(G) = \mathbf{1} = \pi_0(G)$. So if G does not contain any incontractable closed paths and does not have disconnected pieces, then the topologically distinct incontractable paths of G/H are given by the disconnected pieces of H. So one can usually tell that there are strings in a particle physics model simply by checking if the symmetry breaking involves a broken $U(1)$ or if the unbroken group contains a discrete symmetry. This result cannot be applied to the electroweak model since there we have $G = [SU(2) \times U(1)]/Z_2$ and $\pi_1(G) = \mathbf{Z} \neq \mathbf{1}$.

3.2 Example: U(1) local

Consider the Lagrangian

$$L = \frac{1}{2}|D_\mu \Phi|^2 - \frac{1}{4}F_{\mu\nu}F^{\mu\nu} - \frac{\lambda}{8}(\Phi^*\Phi - \eta^2)^2$$

where Φ is a complex field and

$$D_\mu = \partial_\mu - ieA_\mu$$

where, A_μ is an Abelian gauge potential. This model has a U(1) gauge symmetry since it is invariant under

$$\Phi \to e^{i\theta}\Phi \ , \quad A_\mu \to A_\mu + \frac{1}{e}\partial_\mu \theta \tag{64}$$

Now since $\pi_1(U(1)/\mathbf{1}) = \mathcal{Z}$, the model has string solutions labeled by an integer (the winding number).

The string solutions correspond to the non-trivial windings of a circle at spatial infinity on to the vacuum manifold. Therefore the boundary conditions that will yield the string solution will have the form:

$$\Phi(r=\infty,\theta) = \eta e^{in\theta} \ , \quad n \in \mathcal{Z} - \{0\} \tag{65}$$

The gauge fields at infinity must be such that the covariant derivative vanishes there:

$$D_i\Phi = 0 \ , \quad \text{at} \quad r = \infty \ . \tag{66}$$

Let us now construct the string solution using Bogomolnyi's method[1]. The energy for static configurations in two spatial dimensions is

$$E = \int d^2x \left[\frac{1}{2}|D_x\Phi|^2 + \frac{1}{2}|D_y\Phi|^2 + \frac{1}{2}B_z^2 + V(\Phi)\right] \tag{67}$$

with

$$V(\Phi) = \frac{\lambda}{8}(|\Phi|^2 - \eta^2)^2 \tag{68}$$

The trick is to write this as:

$$E = \int d^2x \left[\frac{1}{2}|D_x\Phi \pm iD_y\Phi|^2 + \frac{1}{2}(B_z - \sqrt{2V})^2\right] + \frac{e}{2}\eta^2 \int d^2x B_z \tag{69}$$

in the special case that $\lambda = e^2$ (so called "critical coupling") [a]. The Bogomolnyi equations are:

$$D_x\Phi + iD_y\Phi = 0 \tag{70}$$

$$B_z - \sqrt{2V} = 0 \tag{71}$$

and the energy per unit length of the string is:

$$\mu = \frac{e}{2}\eta^2 \int d^2x B_z = \frac{e}{2}\eta^2 \oint d\theta A_\theta = \pi\eta^2 \ . \tag{72}$$

For non-Bogomolnyi strings, this expression will be multiplied by a factor which depends on λ/e^2. Unless this parameter is very large or small, numerical evaluations show that the numerical coefficient is of order unity.

For strings formed at the Grand Unified phase transition $\eta \sim 10^{16}$ GeV, we find $\mu \sim 10^{22}$ gms/cm which is like the mass of a mountain range packed into a centimeter of string. When calculating the gravitational effects of strings μ always appears in the dimensionless combination $G\mu$. For GUT strings, $G\mu \sim 10^{-6}$.

[a] Unlike in the case of the Z_2 domain wall, the Bogomolnyi trick over here works only for the form of the potential given in eq. (68) and with critical coupling.

3.3 Semilocal and electroweak strings

The standard model symmetry breaking is $SU(2)_L \times U(1)_Y \to U(1)_{em}$ and does not give topological strings. However, it still contains embedded strings which can be perturbatively stable for a range of parameters which are not realized in Nature. In these lectures I will only briefly describe semilocal strings [5].

Consider the generalization of the Abelian Higgs model in which the complex scalar field is replaced by an $SU(2)$ doublet $\Phi^T = (\phi_1, \phi_2)$. The action is

$$S = \int d^4x \left[|(\partial_\mu - iqY_\mu)\Phi|^2 \ - \ \frac{1}{4} Y_{\mu\nu} Y^{\mu\nu} \ - \ \lambda \left(\Phi^\dagger \Phi - \frac{\eta^2}{2} \right)^2 \right] , \qquad (73)$$

where Y_μ is the $U(1)$ gauge potential and $Y_{\mu\nu} = \partial_\mu Y_\nu - \partial_\nu Y_\mu$ its field strength.

This model has symmetry under $G = [SU(2)_{global} \times U(1)_{local}]/Z_2$. Elements of the $SU(2)_{global}$ act on the Higgs doublet, while elements of $U(1)_{local}$ multiply the doublet by an overall phase and transform the gauge field in the usual manner. The action of the center of $SU(2)_{global}$ on the Higgs doublet is identical to a $U(1)_{global}$ phase rotation by π. This is the reason for the Z_2 identification. The model in eq. (73) is just the scalar sector of the Glashow-Salam-Weinberg (GSW) electroweak model with $\sin^2\theta_w = 1$.

Once Φ acquires a vacuum expectation value, the symmetry breaks down to $H = U(1)_{global}$, as in the GSW model. The vacuum manifold is S^3. This may also be seen by minimizing the potential explicitly. The vacuum manifold is described by $\Phi^\dagger\Phi = \eta^2/2$ which is a three sphere. Hence there are no incontractable paths on the vacuum manifold. Yet, it is possible to perform a Bogomolnyi type analysis to find that the configuration:

$$\Phi = f(\rho) e^{i\theta} \begin{pmatrix} 0 \\ 1 \end{pmatrix} \ , \quad Y_\theta = \frac{v(\rho)}{q\rho} \qquad (74)$$

is a solution in cylindrical coordinates (ρ, θ). The profile functions $f(\rho)$ and $v(\rho)$ can be determined by solving the Bogomolnyi equations.

It is also possible to show that the solution is perturbatively stable when $2\lambda < q^2$, neutrally stable at critical coupling $(2\lambda = q^2)$ and unstable for $2\lambda > q^2$.

For the case when the SU(2) is gauged, the string solution continues to exist and can be stable for $\sin^2\theta_w > 0.9$ if the scalar mass is small. In the standard model, however, $\sin^2\theta_w = 0.23$ and the string solution is certainly unstable. Certain external conditions (*eg.* a magnetic field) can stablize the string.

3.4 Formation and evolution

The formation of strings has been studied by numerical methods. Here one throws down $U(1)$ phases on a lattice and checks for topological winding around the plaquettes. If the winding around a plaquette is non-trivial, it means that a string is passing through it. Then the strings are connected and in this way one obtains a network of closed and open strings.

The lattice simulations show several interesting properties of the initial network of strings. First and foremost is the result that most (over 80%) of the string density is in strings that are infinite. Secondly, the string loops occur in a scale invariant distribution – that is, the number density of loops having size between R and $R + dR$ is proportional to dR/R^4, just as would be expected based on dimensional analysis. Thirdly, the long strings have a Brownian shape and so the length l of string in a distance R is given by: $l \propto R^2$.

There has been much effort in extending the lattice simulations to make them more realistic and closer to what might actually happen at a phase transition. However, the essential results of the lattice simulations have held up very well. There has also been a lot of theoretical and experimental effort devoted to determining the density of defects after the phase transition. (In the simulations the density of defects is set by the lattice spacing.) The statistical properties of the network described above are expected to be insensitive to the initial string density. The exact fraction of strings in infinite strings might vary somewhat.

Once the string network has formed, it evolves under the forces that we discussed in the domain wall case: (i) tension, (ii) friction with ambient matter, (iii) Hubble expansion, (iv) intercommuting (reconnection) when strings collide, and (iv) energy loss mechanisms such as gravitational wave emission. Of these factors, frictional forces are important for a short period (for GUT strings) since the Hubble expansion dilutes the ambient matter. The energy loss mechanisms are important but to calculate their effect on the string dynamics is a nasty back-reaction problem. The "zeroth order" factors are the tension, Hubble expansion and intercommutings.

Ignoring friction, energy loss and intercommutings for now, the strings move according to the Nambu-Goto action in a background FRW spacetime:

$$S = -\mu \int d^2\sigma \sqrt{-g^{(2)}} \tag{75}$$

where $g^{(2)}$ is the determinant of the two dimensional string world-sheet metric. If the string worldsheet is written as: $x^\mu(\sigma^a)$ with $a = 0, 1$ where (σ^0, σ^1) are

the worldsheet coordinates, then the worldsheet metric is:

$$g^{(2)}_{ab} = g_{\mu\nu}\partial_a x^\mu \partial_b x^\nu \tag{76}$$

where, $g_{\mu\nu}$ is the four dimensional spacetime metric in which the strings move.

The freedom of choosing coordinates on the worldsheet (reparametrization invariance) can be used to simplify the equations of motion for the string derived from eq. (75). We choose

$$\sigma^0 = \tau \ , \quad \sigma^1 = \zeta \tag{77}$$

where ζ is a parameter along the string at any given instant of the conformal time τ (see eq. (6)). Then the equation of motion is:

$$\ddot{\mathbf{x}} + 2H(1-\dot{\mathbf{x}}^2)\dot{\mathbf{x}} = \epsilon^{-1}\left(\frac{\mathbf{x}'}{\epsilon}\right)' \tag{78}$$

where overdots refer to derivatives with respect to τ and primes with respect to ζ.

The equation of motion for a single string allows numerical evolution of the network of strings but does not take intercommutings into account. In practice, the network is numerically evolved until two strings intersect and then the reconnection is done by hand.

To study the evolution of cosmic strings by solving the equations of motion is similar to studying a box of gas by solving Newton's equations of motion for each particle in the box and taking care of collisions by hand. For almost all cosmological purposes, only the statistical properties of the string network are relevant. So one should define "statistical variables" and find their evolution. The one scale model for string evolution is precisely such an attempt.

3.5 One scale model

As the name suggests, the "one scale model" is based on the assumption that there is only one length scale that characterizes the infinite strings in the network [6,7]. (The short loops are considered separately.) If we denote this scale by L then the distance between strings and the correlation length of a single string (the distance out to which it is straight) are both given by L. With time L can change and hence we need to derive an equation for $L(t)$.

The usual way of defining the length L is by considering the total energy E in strings lying inside a volume V. Then

$$\rho \equiv \frac{E}{V} \equiv \frac{\mu}{L^2} \tag{79}$$

defines L. The energy changes with time since the Hubble expansion dilutes and stretches the string network. Also, the velocity of a string redshifts due to the Hubble expansion. Long strings also lose energy by self-intersecting to form short loops. This gives

$$\dot{\rho} = -2H(1 + v_{rms}^2)\rho - c\frac{\rho}{L} \tag{80}$$

where

$$v_{rms}^2 \equiv \langle v^2 \rangle = \frac{\int d\zeta \epsilon \dot{\mathbf{x}}^2}{\int d\zeta \epsilon} \tag{81}$$

is the average rms velocity of strings and c is a parameter that accounts for the frequency of self-intersection (the so called "chopping efficiency"). Equation (80) can also be written as an equation for L:

$$\dot{L} = HL(1 + v_{rms}^2) + \frac{c}{2} \tag{82}$$

(Since the chopping term must vanish if the velocity of the strings vanishes, one frequently writes $c = \tilde{c} v_{rms}$.)

The network is said to scale if, at every epoch, the network has the same statistical properties. Hence the scale L should be a fixed fraction of the horizon size t. In this case, the energy density ρ in long strings will fall off like $1/t^2$, exactly as the total matter density does in a radiation or matter dominated universe. In a universe with a cosmological constant, scaling will hold in a trivial sense since the rapid expansion will dilute the strings to vanishing energy density. Scaling will not hold in the epochs during the period in which the universe changes from being radiation dominated to matter dominated, or from matter dominated to cosmological constant dominated. Both these transitions are relevant for examining the cosmological signatures of strings (*eg.* the cosmic microwave background anisotropies), making the problem quite hard.

To check for scaling we write

$$L = \gamma(t)t \ , \tag{83}$$

insert this relation into eq. (80) to get

$$\frac{\dot{\gamma}}{\gamma} = \frac{1}{t}\left[\frac{c}{2\gamma} - \{1 - Ht(1 + v_{rms}^2)\}\right] \tag{84}$$

There is a fixed point solution ($\dot{\gamma} = 0$) at the point:

$$\gamma = \frac{c}{2}\frac{1}{1 - (Ht)(1 + v_{rms}^2)} \ . \tag{85}$$

Note that for a power law expansion Ht does not depend on time. The rms velocity could depend on time though we can prove that $v_{rms}^2 = 1/2$ in flat spacetime suggesting that it may be a reasonable assumption to take it to be roughly constant even in the expanding universe. However, we can derive an equation for v_{rms} by differentiating eq. (81) with respect to time and then using the equation of motion. This gives

$$\dot{v}_{rms} = (1 - v_{rms}^2)\left[\frac{k}{L} - 2Hv_{rms}\right] \tag{86}$$

where k is a parameter (the "momentum parameter") related to the typical radius of curvature of the strings. The second term gives the redshifting of the velocity due to Hubble expansion while the first describes the change in the velocity due to the tension in the string.

Equation (82) and (86) are the one scale model equations for the string network. These equations depend on the chopping efficiency c (or $\tilde{c}$) and the momentum parameter k that need to be specified. The practice has been to use the values found in numerical simulations. Martins and Shellard [8] give

$$\tilde{c} = 0.23 \pm 0.04 \tag{87}$$

and a velocity dependent value of k

$$k(v) = \frac{2\sqrt{2}}{\pi}\frac{1 - 8v^6}{1 + 8v^6} \tag{88}$$

4 Cosmological constraints and signatures

Numerical evidence suggests that the density of strings scales with the expansion of the universe and so we have: $\rho \sim \mu/t^2$. Compared to the critical density in a radiation- or matter-dominated universe $\rho_c \sim 1/Gt^2$, the string density is at least a factor $\sim G\mu$ smaller at all times. So the strings never come to dominate the universe.

4.1 CMB and P(k)

The energy-momentum of the network of strings causes perturbations in the metric which can introduce fluctuations in the cosmic microwave background. The metric produced by a straight string is conical with deficit angle $8\pi G\mu$ and photons arriving to us from either side of a moving string have a temperature difference of $\sim 8\pi G\mu v$ where v is the velocity component of the string transverse to the direction of propagation of the photons. Therefore, on dimensional

grounds, the CMBR anisotropy produced by strings is:

$$\frac{\delta T}{T} \sim 8\pi G\mu \tag{89}$$

which for GUT strings is about what is observed.

Several sophisticated calculations of the CMBR anisotropy induced by strings have been done. I would like to draw a distinction between some of the analyses that have been done for global strings and others that have been done for local strings. Here I will only discuss the specific analysis done by Pogosian and me of CMBR anisotropies produced by local strings [9].

First of all we need to find the energy-momentum tensor of the string network as it evolves over time. For this we adopt a model first developed by Albrecht, Battye and Robinson [10]. The string network at any time is taken to be a gas of straight string segments of length L and moving with velocity v_{rms}. Then we evaluate the energy-momentum tensor of the network. For the evolution, we follow the one-scale model described earlier. A tricky part of the problem is to allow some of the strings to decay. This is done by eliminating some of the segments with time in such a way as to preserve the scaling form of the string energy density. Once the energy-momentum of the string network is obtained, we feed it into the program CMBFAST to evaluate the anisotropy and also the power spectrum of density fluctuations.

Some of the results are shown in Fig. 2. (I am assuming that you have already been introduced to the theory behind the microwave background measurements.) Clearly there is only one Doppler peak and it occurs at $l \sim 400$ and this does not agree with observations.

It is known that larger values of Ω bring down the position of the Doppler peak. So Pogosian has recently investigated local strings in a closed model [11]. The result that the peak position only scales as $\Omega^{-1.58}$ would seem to imply that we would need to go to $\Omega \sim 3$ in order to bring down the peak position by a factor of two or so. However, this result does not apply to perturbation sources such as cosmic strings where the anisotropy is affected by the gravitational potentials produced after last scattering. Simulations by Pogosian [11] show that the peak position shifts to $l \sim 200$ for $\Omega \simeq 1.3$ (see Fig. 3). Furthermore, the closest fit to the data occurs for $G\mu = 1 - 2 \times 10^{-6}$. While this matches the GUT scale, the poor fit to the data means that GUT strings cannot be solely responsible for producing the required density inhomogeneities.

4.2 Gravitational wave background

When local strings oscillate at very low frequencies, they can only radiate very low energy particles. Frequencies set by cosmic scales are $\sim 1/t$ and the

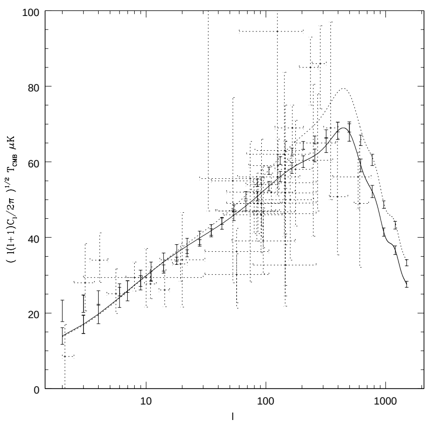

Figure 2: The spectrum of microwave background fluctuations for the network of wiggly strings with $L = 0.1$. The solid and dotted lines correspond to two values of the network parameters. The observations with error bars are also shown.

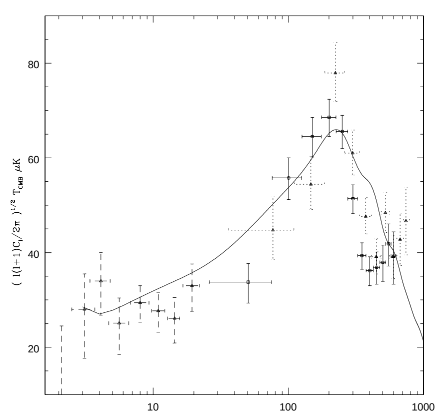

Figure 3: As in Fig. 2 but for a closed universe with $\Omega = 1.3$. See the article by *Pogosian* [11] for fuller account of the parameters used and the underlying assumptions.

only known particles that can be radiated are massless - photons and gravitons. (Neutrinos are assumed to have a non-zero mass.) Generally the (local) strings are made of neutral fields and hence do not radiate significantly in photons [b]. Then the primary decay channel for strings is into gravitons [c].

To estimate the power emitted in gravitational radiation by a string loop of length L, it is most convenient to use the quadrupole formula. The only dimensional parameters available to us are G, μ and L. However, we know that the power loss into gravitational waves is proportional to one factor of G and two factors of μ since the power is the square of the quadrupole moment. Now since the power has dimensions of mass squared, we must have

$$P \sim G\mu^2 \tag{90}$$

and the length of the loop drops out from the estimate. In the cosmic scenario we are interested in the average gravitational energy emitted per unit time by all strings. So we write:

$$\bar{P} = \Gamma G\mu^2 \tag{91}$$

where Γ is a numerical factor. By examining the power emitted by many different loops, one finds $\Gamma \sim 100$ [12].

To find the present gravitational wave background amplitude and spectrum one needs to sum over all strings in the network, include appropriate redshift factors etc.. The final result is [13]:

$$\Omega_g(\omega) = \frac{18\pi^2(\beta-1)^2\nu G\mu}{(3-\beta)\sin[(2-\beta)\pi]}\left(\frac{4\pi}{\Gamma\mu\omega t_0}\right)^{\beta-1} \tag{92}$$

where ν is a parameter that sets the amplitude for the number density of loops and $4/3 \leq \beta << 2$ is a parameter that characterizes the typical spectrum of gravitational radiation emitted by loops, t_0 is the present epoch. The peak of the spectrum is at

$$\omega_{peak} \sim \frac{4\pi}{\Gamma G\mu t_0}\ . \tag{93}$$

The strongest constraints on the amplitude of the gravitational wave background arise from the timing of the millisecond pulsar. In 1993 the constraint was:

$$\Omega_g < 4 \times 10^{-7} h^{-2} \tag{94}$$

---

[b] If the strings are superconducting they may carry electrical charges and currents, and then they would lose energy by emitting photons.

[c] Global string loops decay primarily by emitting Goldstone bosons.

The constraint gets more stringent the longer the millisecond pulsar is observed without encountering noise in its timing. Today the constraint would be slightly stronger than in 1993. In terms of $G\mu$, this gives

$$G\mu < 4 \times 10^{-5} \tag{95}$$

The emission of gravitational radiation from strings also contributes to the energy density prior to nucleosynthesis. If the gravitational radiation contribution to the content of the universe exceeds about 5% , it will interfere unacceptably with BBN. This gives another constraint on the parameter $G\mu$ that is slightly better, though comparable to, the one in eq. (95).

4.3 Gravitational lensing

Spacetime distortions due to cosmic strings would lead to gravitational lensing of background sources. The angular separation of images can be deduced from the value of the conical deficit angle to be:

$$\delta\phi = 8\pi G\mu \frac{d}{d+l} \tag{96}$$

where d is the distance between the source and the string and l is the distance between string and observer. This leads to an image separation of about 5 arc sec from GUT strings and is quite large by astronomical standards.

Initially it was thought that a string would produce a line of lensed images of sources and this would be a unique signature. However, since the strings are wiggly, this conclusion is no longer obvious. Instead one needs to examine the lensing of sources due to a more realistic (wiggly) string. This was done by *de Laix et. al.* [14] and the results are shown in Fig. 4.

4.4 Other signatures

Cosmic strings and other topological defects have been considered as sources for ultra high energy cosmic rays and gamma ray bursts.

5 Zero modes and superconducting strings

The interaction of fermions with strings can often lead to "zero modes" *i.e.* zero energy solutions to the Dirac equation in the string background. If these fermions carry electric charge, electric fields along the string (equivalently, string motion through a magnetic field) can produce electric currents on the string which will persist even when the electric field is turned off. Hence such strings are said to be "superconducting".

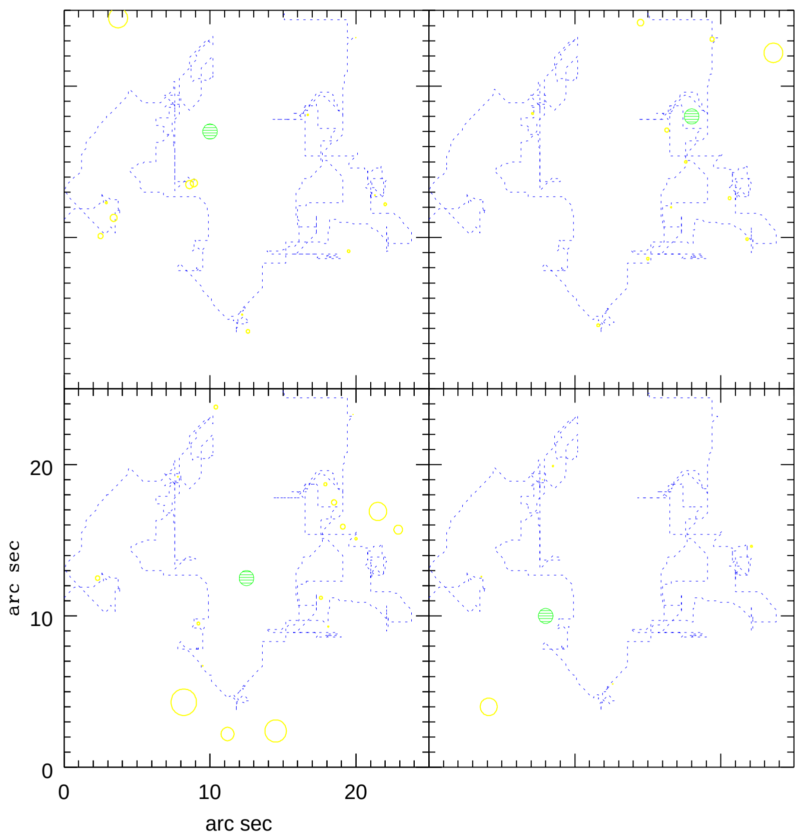

Figure 4: The projection of a long wiggly string on the sky is shown together with a variety of point sources (hatched circles). The images of the point sources are shown as unfilled circles.

The current on a superconducting string depends on the initial current on it at formation and also on the flux of magnetic field that it has traversed. The motion of the current carrying string leads to electromagnetic radiation that can dissipate the string energy. At the same time, the electromagnetic radiation can cause spectral distortions in the cosmic microwave background. This places constraints on the density of superconducting strings in the early universe and also the amount of current on them if they exist.

6 Magnetic monopoles

6.1 Topology: π_2

Magnetic monopoles are formed when the vacuum manifold has incontractable two spheres. The relevant homotopy group is $\pi_2(G/H)$. As discussed in the string case, if $\pi_2(G) = \mathbf{1} = \pi_1(G)$, then

$$\pi_2(G/H) = \pi_1(H) \ . \tag{97}$$

Hence we get magnetic monopoles whenever the *unbroken* group contains incontractable paths. We know that today the unbroken group contains the U(1) electromagnetic gauge symmetry which contains incontractable paths. Hence, any GUT predicts magnetic monopoles.

6.2 Example: SU(2)

The 't Hooft-Polyakov monopole is based on an SU(2) model:

$$L = -\frac{1}{4} X^a_{\mu\nu} X^{a\mu\nu} + \frac{1}{2}(D_\mu \Phi^a)^2 - V(\Phi) \ , \tag{98}$$

where Φ is an SU(5) adjoint scalar field, $X^a_{\mu\nu}$ $(a = 1, ..., 24)$ are the gauge field strengths and the covariant derivative is defined by:

$$D_\mu \Phi^a = \partial_\mu \Phi^a - ie[X_\mu, \Phi]^a \tag{99}$$

and the group generators are normalized by $\mathrm{Tr}(T_a T_b) = \delta_{ab}/2$. Once Φ acquires a VEV, the symmetry is broken down to U(1), consisting of SU(2) rotations that leave Φ invariant.

It is possible to give a Bogomolnyi type derivation of the monopole solution in the case that the potential vanishes *i.e.* $V(\Phi) = 0$. The explicit solution in spherical coordinates is [15]:

$$\Phi = \frac{1}{er^2}\left(\frac{Cr}{\tanh(Cr)} - 1\right) x^a T_a \tag{100}$$

$$W^a_i = \epsilon^a{}_{ij}\frac{x^j}{er^2}\left(1 - \frac{Cr}{\sinh(Cr)}\right) \ .(a,i,j = 1,2,3) \ , \tag{101}$$

This $V = 0$ monopole is referred to as the Bogomolnyi- Prasad-Sommerfield (BPS) monopole. For $V \neq 0$, the profile functions can be found numerically.

The mass of the BPS monopole also follows from the Bogomolnyi analysis and is:

$$M = \frac{4\pi}{e^2} m_V \tag{102}$$

where m_V is the mass of the massive vector bosons after symmetry breaking. In terms of the vacuum expectation value η of Φ, $m_V = e\eta$.

6.3 Electroweak monopoles

The standard electroweak model does not contain the suitable topology to have magnetic monopole solutions. This is because $\pi_1(G) \neq \mathbf{1}$ and the incontractable loops in the unbroken U(1) are also incontractable in G. Yet, as originally discovered by Nambu[16], the model does contain magnetic monopoles that are confined by strings. (This is closely analagous to the picture of quarks being confined by QCD strings.)

The standard model has a doublet Φ, SU(2) gauge fields W^a_μ and the hypercharge gauge field Y_μ. The SU(2) and U(1) coupling constants are denoted by g and g' and the vacuum expectation value of Φ is denoted by η. The weak mixing angle θ_w is defined via $\tan\theta_w = g'/g$. The asymptotic configuration of the electroweak monopole can be written in spherical coordinates (with $r \to \infty$) as:

$$\Phi = \frac{\eta}{\sqrt{2}}\begin{pmatrix} \cos(\theta/2) \\ \sin(\theta/2)e^{i\varphi} \end{pmatrix} \tag{103}$$

$$gW^a_\mu = -\epsilon^{abc} n^b \partial_\mu n^c + i\cos^2\theta_w n^a (\Phi^\dagger \ \partial_\mu \Phi - \partial_\mu \Phi^\dagger \ \Phi) \tag{104}$$

$$g' Y_\mu = -i\sin^2\theta_w (\Phi^\dagger \ \partial_\mu \Phi - \partial_\mu \Phi^\dagger \ \Phi) \tag{105}$$

where

$$n^a(x) \equiv -\frac{\Phi^\dagger(x)\tau^a\Phi(x)}{\Phi^\dagger(x)\Phi(x)} \ . \tag{106}$$

Note that the configuration has a singularity along the negative z axis – the lower component of Φ is not single-valued here. This is the location of a real string. As described in Sec. 3.3, this string is the semilocal string when $\theta_w = \pi/2$ and the electroweak Z-string for general θ_w.

The electroweak monopole is not a static *solution* of the equations of motion but only a field configuration. One way to see this is that to note that the

Table 2: The quantum numbers (n_8, n_3 and n_1) on stable $SU(5)$ monopoles are shown and these correspond to the $SU(3)$, $SU(2)$ and $U(1)$ charges on the corresponding standard model fermions shown in the right-most column.

n	$n_8/3$	$n_3/2$	$n_1/6$	
+1	1/3	1/2	1/6	$(u,d)_L$
-2	1/3	0	-1/3	d_R
-3	0	1/2	-1/2	$(\nu,e)_L$
+4	1/3	0	2/3	u_R
-6	0	0	-1	e_R

string is pulling on the monopole and this unbalanced force will tend to accelerate the monopole and to shorten the string. Eventually the monopole will annihilate the antimonopole at the other end of the string. However this fact may not diminish the importance of the monopole – the important aspect to consider is the lifetime of the electroweak monopole and antimonopole and to evaluate if they can lead to some experimental signatures [16]. At the moment, it seems unlikely that the electroweak monopole can survive long enough to be seen in accelerator experiments though this issue needs further exploration.

6.4 SU(5) monopoles

The Grand Unified symmetry breaking $SU(5) \to [SU(3) \times SU(2) \times U(1)]/Z_6$ leads to topological magnetic monopoles. The magnetic monopoles in this model have been constructed [17]. Here I will not go into the details of the construction. Instead I will only point out an interesting feature of the spectrum of stable magnetic monopoles.

The winding one monopole in the model has SU(3), SU(2) and U(1) charges. Then one can construct higher winding monopoles by assembling together unit winding monopoles. In some cases, the assembly will be stable while in other cases the higher winding monopole will be unstable to decaying into lower winding monopoles. It turns out that, for a broad range of parameters, the stable monopoles are the winding ± 1, ± 2, ± 3, ± 4, and ± 6 monopoles. The magnetic charges on these can be calculated. As shown in Table II an interesting feature is that the known quarks and leptons have precisely the same spectrum of charges in the electric sector! This observation has led to the possibility that it might be possible to understand the fundamental particles as magnetic monopoles [18].

6.5 Cosmology of monopoles

Once magnetic monopoles are produced at a phase transition in the early universe, their energy density will redshift like pressureless matter $\rho_m \propto 1/a^3$. The radiation redshifts as $\rho_\gamma \propto 1/a^4$. Hence magnetic monopoles will start dominating the universe at some epoch. The exact epoch of domination will depend on the details of monopole formation and their evolution. However, even if we assume one monopole per causal horizon at formation, GUT monopoles would have started dominating well before big bang nucleosynthesis, which is clearly in conflict with observations [19,20].

Another bound on the monopole density arises from the observation that galaxies have magnetic fields that would accelerate any magnetic monopoles that are present. In this way the monopoles would dissipate the magnetic field. This "Parker bound" leads to a constraint that is stronger than the cosmological constraint for lighter monopoles [21].

The present constraints on monopoles imply that magnetic monopoles must be more massive than about 10^{10} GeV if they are to be present in cosmology. For certain types of monopoles (*eg.* those that catalyse proton decay), the constraints from stellar physics can be much stronger.

The constraints on magnetic monopoles are clearly in conflict with the result that the GUT phase transition must have produced magnetic monopoles. Hence either the GUT philosophy is incorrect, or the standard FRW cosmology is incorrect. The popular solution to the monopole over-abundance problem is that the standard cosmology should be modified to include an inflationary phase of the universe. Then the monopole producing GUT phase transition occurs during the inflationary stage and any monopoles that were produced are rapidly diluted to insignificant densities. Other possible solutions are to (i) modify particle physics such that the monopoles get connected by strings and then annihilate, [22] (ii) never have an epoch where the Grand Unified symmetry is restored [23], and (iii) produce domain walls that sweep away the monopoles [2].

7 Further reading

The topological defects literature is vast and the citations have not done justice to all the work that has been done. Fortunately a number of excellent review articles and books have been written that can be a guide to the original literature. Here are some of these articles:

- "Solitons and Particles", eds. C. Rebbi and G. Soliani (World Scientific, Singapore, 1984). This is an invaluable resource for learning the subject

and for reading most of the classic papers on the field theoretic aspects.

- "Cosmic Strings and Other Topological Defects", A. Vilenkin and E.P.S. Shellard, Cambridge University Press (1994). This is a comprehensive description of the field.
- M.B. Hindmarsh and T.W.B. Kibble, Rept. Prog. Phys. **58**, 477 (1995). An excellent discussion of the many different facets of cosmic strings.
- P. Goddard and D. I. Olive, Rep. Prog. Phys. **41** 1357-1437 (1978). A classic on magnetic monopoles.
- S. Coleman, "The magnetic monopoles, fifty years later", in: The Unity of Fundamental Interactions, ed A. Zichichi (Plenum, London, 1983). Another classic.
- J. Preskill, "Vortices and monopoles", in: Architecture of Fundamental Interactions at Short Distance, eds P. Ramond and R. Stora (Elsevier, 1987). And yet another.
- "Semilocal and Electroweak Strings", A. Achúcarro and T. Vachaspati, Phys. Rep. **327**, 347 (2000).
- "Aspects of ^{3}He and the Standard Electroweak Model", G.E. Volovik and T. Vachaspati, *Int. J. Mod. Phys.* **B10** 471-521 (1996). A review of topological defects in He-3 with a particle physics connection.

Acknowledgements

This work was supported by the Department of Energy, USA.

References

1. E. B. Bogomolny, Sov. J. Nucl. Phys. **24** 449 (1976); reprinted in "Solitons and Particles", eds. C. Rebbi and G. Soliani (World Scientific, Singapore, 1984).
2. G. Dvali, H. Liu and T. Vachaspati, Phys. Rev. Lett. **80**, 2281 (1998).
3. L. Pogosian and T. Vachaspati, Phys. Rev. **D62**, 123506 (2000).
4. T. Vachaspati and A. Vilenkin, Phys. Rev. **D30**, 2036 (1984).
5. T. Vachaspati and A. Achúcarro, *Phys. Rev.* **D44**, 3067 (1991).
6. T.W.B. Kibble, Nucl. Phys. **B261**, 750 (1985).
7. D.P. Bennett, Phys. Rev. **D33**, 872 (1986); Erratum: Phys. Rev. **D34**, 3932 (1986).

8. C. J. A. P. Martins and E. P. S. Shellard, hep-ph/0003298 (2000).
9. L. Pogosian and T. Vachaspati, Phys. Rev. **D60**, 083504 (1999).
10. A. Albrecht, R. Battye and J. Robinson, Phys. Rev. **D59**, 023508 (1999).
11. L. Pogosian, astro-ph/0009307 (2000).
12. T. Vachaspati and A. Vilenkin, Phys. Rev. **D31**, 3052 (1985).
13. R.R. Caldwell and B. Allen, Phys. Rev. **D45**, 3447 (1992).
14. A.A. de Laix, L.M. Krauss and T. Vachaspati, Phys. Rev. Lett. **79**, 1968 (1997).
15. M.K. Prasad and C.H. Sommerfield, Phys. Rev. Lett. **35**, 760 (1975).
16. Y. Nambu, Nucl. Phys. **B130**, 505 (1977).
17. C.P. Dokos and T.N. Tomaras, Phys. Rev. **D21**, 2940 (1980).
18. T. Vachaspati, Phys. Rev. Lett. **76**, 188 (1996).
19. Ya.B. Zeldovich and M.Yu. Khlopov, Phys. Lett. **B79**, 239 (1978).
20. J. Preskill, Phys. Rev. Lett. **43**, 1365 (1979).
21. E.N. Parker, Ap. J. **160**, 383 (1970).
22. P. Langacker and S.-Y. Pi, Phys. Rev. Lett. **45**, 1 (1980).
23. G. Dvali, A, Melfo and G. Senjanovic, Phys. Rev. Lett. **75**, 4559 (1995)